

## Influence of Geometric Simplifications on Lightning Strike Simulations

Guadalupe G. Gutierrez<sup>1, \*</sup>, Sergio F. Romero<sup>2</sup>, Monica Gonzaga<sup>3</sup>, Enrique Pascual-Gil<sup>1</sup>, Luis D. Angulo<sup>4</sup>, Miguel R. Cabello<sup>4</sup>, and Salvador G. Garcia<sup>4</sup>

**Abstract**—This paper discusses the influence of simplifications in models used in the design of electromagnetic protection against indirect effects of lightning strikes. A real and complex test case such as the power plant of an A400M aircraft, simulated with the FDTD method, is chosen for this. The parameters studied are the inclusion/removal of installations, modification of electrical contacts, material properties, and changes in the cable characteristics. The simulations performed allow us to quantify the impact of different simplification approaches and, in consequence, to draw conclusions on the relative importance of different model features, being the most important ones to maintain the electrical contacts, to include installations and cables carrying high currents, to consider different materials, to respect the accurate cable routes or to take care of isolated equipment.

### 1. INTRODUCTION

A commercial aircraft is subject to at least one lightning strike per year [1]. The effects of these strikes can be categorised into two kinds of damaging effects: direct or indirect [1]. Direct effects consist of physical damage to the structure due to direct attachment or to current flow. Indirect effects, on which we focus this study, are generated by voltage and current transients in the electrical wiring. These transients are caused by the electromagnetic (EM) field created by the lightning current which flows along the aircraft surface. This EM field penetrates the fuselage through apertures such as windows or by diffusion through parts made of composite materials. Inside the aircraft, these transients can overcome the immunity limit of the equipment, generating failures and/or damage, compromising aircraft safety. Among the indirect effects, the most significant parameters are rates of current rise and decay, and peak amplitude [2–5]. The aim of lightning protection is to prevent catastrophic accidents arising from a lightning strike, to ensure a safe flight and landing [1, 2, 6, 7].

Computational electromagnetic (CEM) tools can help predict the response of a complex structure. A wide variety of algorithms and methods have been developed to address the electrically large problems that are often encountered in the aircraft industry. This advance, together with the exponential growth of computational capabilities, makes it possible to estimate transfer functions between a lightning strike and internal fields or the currents induced on bundles in a complete aircraft. These methods can be applied during the certification process and the life-cycle of an aircraft, thus increasing flight safety. CEM methods also make it possible to carry out parametric studies during the design phase, when changes are simpler and less costly. However, the development of suitable EM models for complex structures is a time-consuming process. As a first step, a geometric simplification is needed, since the full digital mock-up cannot be directly managed by EM simulators. This simplification is a crucial task, which usually implies the elimination of very small parts and details, such as holes, bolts and nuts,

---

*Received 10 January 2018, Accepted 17 March 2018, Scheduled 4 April 2018*

\* Corresponding author: Guadalupe Gutierrez Gutierrez (guadalupe.gutierrez@airbus.com).

<sup>1</sup> Airbus Defence and Space, Getafe, Spain. <sup>2</sup> INTA, Torrejon de Ardoz, Spain. <sup>3</sup> CT Ingenieros, Getafe, Spain. <sup>4</sup> Department of Electromagnetism, University of Granada, Granada, Spain.

and may also call for surfaces to be redefined [8, 9]. The analysis of uncertainties associated with this process is currently the focus of much research attention. Statistical methods dealing with uncertainties in the parameters of cables, materials, circuits, etc., such as those based on Monte Carlo analysis or on stochastic Finite Difference Time Domain (FDTD) modelling [10, 11], are still either computationally prohibitive or too limited, to be applied to the complexity of a modern aircraft. For this reason, the engineer's experience in managing the information included in the digital mock-up plays a fundamental role in the success of this process.

This paper contributes to our understanding of these questions by quantifying the impact of different simplification approaches, in order to enrich the few literature that can be found on this subject. To do so, we employ a test case based on the power plant of the A400M aircraft [12] to assess which parameters are most influential in an EM simulation, by conducting a heuristic approach based on an affordable set of simulations chosen as representative according to our engineering experience. In particular, we study the inclusion of installations (that is, physical structures needed to install the systems in the aircraft for their correct support and operation), the maintenance of electrical contacts, the assignation of materials, and the selection of appropriate cables with their significant properties. We then estimate the sensitivity of these simulation results to variations in the EM model. Theoretical guidelines are provided, and, in addition, a quantitative notion of the error magnitude which is made with these approximations. The factors which should be taken into account in a 3D EM model for lightning indirect effects are analyzed using this real and complex test case, so as to quantify their influence in the simulation results. Other factors are revealed as not important for this kind of simulations.

The rest of the paper is organized as follows. In Section 2, the model of the power plant is described, and the features of the simulations performed are explained. Section 3 presents the results obtained and discusses the modifications taken into account. Finally, in Section 4, we draw the main conclusions of our analysis.

## 2. SIMULATION DETAILS

### 2.1. Model Details

The EM model of the A400M power plant represented in Fig. 1 was selected for our parametric study for two main reasons: it is a very complex and complete model, which allows us to perform most of the modifications needed for this study, and its size is affordable, and so a large number of simulations

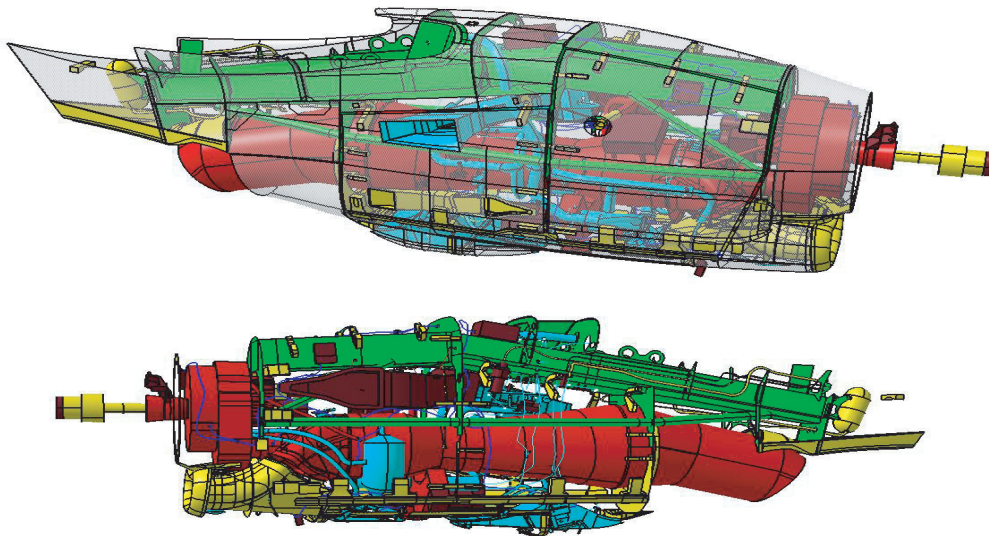


**Figure 1.** A400M power plant EM model (carbon fibre nacelle shown in white with a degree of transparency; the metallic nacelle is in yellow, the mounting is in green, the engine is in red, the equipment is in brown, the systems are in cyan and the harnesses are in dark blue).

can be performed. The power plant has three main structural components: the engine, the mounting and the nacelle. The lightning channel, represented by a nodal electric current density source [13], was chosen to impact the power plant at the nose and to exit it via the mounting to the wing, which is one of the most common situations. In this configuration, the mounting is the principal massive metallic structure along which the current flows. The nacelle includes the fairings, which are mainly made of carbon fibre composite (CFC). For the reference model used in our comparisons, all the equipment and installations are included. The total length of the power plant is around 6 m.

Four overbraided harnesses were included in the model to analyse the currents induced on them. They have been especially selected between the real harnesses of the power plant to cover the different zones of the model. Their description is as follows:

- The Controller Area Network bus (CANBUS) harness has 17 branches, with sizes from 300 to 1500 mm, that interconnect 10 items of equipment around the engine.
- The Electronic Control Unit (ECU) and the Air Cooled Oil Cooler (ACOC) Actuator are connected through the ECU-ACOC harness. This is a simple cable with no branches, about 4 m long.
- The H502 harness connects two fire detection sensors located in the nacelle and extends 6 m across the lower fairing, with no branches.
- PBCU-FW is a harness with 7 branches, measuring no more than 600 mm, located between the mounting and the upper fairing. It connects the Propeller Brake Control Unit (PBCU) with the firewall (FW) to the wing.

## 2.2. Simulation Description

We analyse the induced current response to a severe first return stroke of a lightning bolt. This waveform (WF A) consists of a double exponential with 200 kA peak current and around 6.4  $\mu$ s rise time [14]. In August 2008, IEEE issued a standard defining the Feature Selective Validation (FSV) technique for the comparison of different traces in CEM [15–17]. However, in this work, we have focused the study in analysing the main parameters which must be considered in order to provide an aircraft with lightning strike protection in compliance with international certification requirements. Both time and frequency domains are analysed, since they contain different information: peak amplitude and time to peak (time interval from the start of the simulation until the peak is reached) are, in general, straightforward to analyse in the time domain, while main resonances are more easily analysed in the frequency domain. In the time domain, a Gaussian derivative, shorter than WF A but covering the same spectral range, was used as an excitation waveform, and the results obtained were transformed into WF A response. For the reference configuration, the simulation using directly the WF A has been performed, leading to exactly the same peak currents and times to peak, which are the values analysed in the present study. In the frequency domain, a Gaussian waveform was used to excite the structure so as to reach frequencies up to 50 MHz, which were taken as the upper limit of a lightning strike excitation.

In this study, two kinds of observables were considered:

- 26 probes for the currents induced at each cable branch: 17 from the CANBUS harness, 1 from ECU-ACOC, 1 from H502 and 7 from the PBCU-FW harness. These probes measure the current at particular thin wire nodes [18]. As typical in EMC testing, current probes were placed at a distance of 50 mm from the harness end for ending branches [19], and in the middle of the branch for the intermediate branches.
- Bulk current probes at the 6 main installations, to determine the current that flows across their surfaces. They compute the currents within an integral contour utilizing Ampere's law [20].

The actual transient level (ATL), which reflects the current and voltage waveforms and levels that are induced on the aircraft at the port of the cable networks, is determined from simulations [3–5, 14, 19], and leaves little margin for errors or tolerances. In our study, differences of over 1 dB (12.2% error) were considered significant.

A Cartesian FDTD mesh with a constant space-step of 10 mm, small enough to solve the frequencies of interest and to represent the details of the A400M PWP, while big enough to lead to affordable simulations, was employed for the simulations. Mur's [21] absorbing boundary conditions, computationally lighter than those based on the perfectly matching layer condition [22], were employed

to truncate the domain, yielding a problem size of around 100 Mcells. A time-step of 15 ps was employed to meet the Courant-Friedrichs-Lewy (CFL) stability condition [22]. A total time of 10  $\mu$ s was simulated, which was sufficient to obtain reasonable convergence of the currents. A computation time of approximately 46 hours, using 2 Intel Xeon eight-core 2.9 GHz nodes with 128 GB of memory (400 Mcells/s), was required for each configuration.

### 2.3. Simulation Tools

Several EM simulation tools can be used in the design of protection against lightning strikes. Of these, we selected the one based on the FDTD technique [22] as the most suitable method for this kind of problem, as it obtains the solution in the whole frequency range with a single execution. In this study, the 3D CAD CATIA V5 R21 [23], FDTD mesher CADfix V8.1 SP2.0 64 bit [24], and FDTD solver UGRFDTD R2660 [25] were used to generate the simplified CAD, to mesh it and to simulate it, respectively.

CADfix allows the user to mesh the region where EM propagation is to be calculated. It serves as a graphical user interface which can import data from computer-aided design (CAD) models. All relevant EM properties (permittivity, permeability, impedance, etc.) can be defined, together with the boundary conditions, mesh density, probe locations, etc. CADfix generates a text file containing all the information needed to specify the problem, and this can provide the input to UGRFDTD. This solver is a state-of-the-art parallel 3D full-wave EM simulation tool which uses the FDTD method [22, 26], combined with a multiconductor transmission line (MTLN) solver [27] to address the cabling. It has been developed by UGR in collaboration with Airbus Defence and Space within several research and technology projects [28, 29]. It is especially suited to deal with HIRF/Lightning/NEMP electrically-large EMC problems [30–33], and can account for complex structures, materials, cables, composite thin-panels, etc. A variety of output data can be obtained including the electric current and voltage transient profiles stressing electric/electronic equipment considered in this study.

## 3. ANALYSIS OF RESULTS

Four different kinds of tests were analysed. The main results from the most conclusive cases are presented and explained in this section. In the following tables,  $\Delta$  (dB),  $\Delta$  or  $\Delta_{peak}$  (dB) stand for the amplitude differences in dB between the peak current in the modified model with respect to the reference model, and  $\Delta t$  ( $\mu$ s) or  $\Delta t$  stand for the differences in  $\mu$ s between the time to peak in the modified model with respect to the reference model.

### 3.1. Removal of Components

Since the geometric simplification is extremely time consuming (it can require years for a complete aircraft), when a complex geometry is to be simplified, it is important to know which components (equipment, systems, installations, etc.) are relevant for the model. To assess the effects of their removal, we carried out simulations and studied the peak currents induced. The differences observed with respect to the reference model are shown in Table 1.

#### 3.1.1. Removal of Oil System (OILS)

The OILS is located far from the majority of cable branches but in electrical contact with ACOC, which is one termination of the ECU-ACOC harness (Fig. 2). The currents in two branches, ECU-ACOC and CANBUS-15, change significantly after this removal. The change in the ECU-ACOC harness could have been estimated *a priori* as the ACOC system is in electrical contact with the OILS. Less obvious is the variation in the current induced along the CANBUS-15. This is explained by two facts. Firstly, this branch ends at ECU and runs parallel to the ECU-ACOC cable, and so there is a large mutual inductance. Secondly, as shown below, significant variations are almost always observed in the currents at CANBUS-15, whatever the modification made to the model, because its current is very low, and so any variation is very noticeable. Moreover, many modifications in the model can produce a change in the waveform within this cable, significantly affecting its peak current. However, this is not always

**Table 1.** Removal of components.

| Branch     | OILS<br>$\Delta(\text{dB})$ | IPSA<br>$\Delta(\text{dB})$ | Systems<br>$\Delta(\text{dB})$ |
|------------|-----------------------------|-----------------------------|--------------------------------|
| CANBUS-1   | 0.0                         | 0.0                         | 1.1                            |
| CANBUS-2   | 0.0                         | 0.0                         | 1.0                            |
| CANBUS-3   | 0.0                         | 0.0                         | 1.0                            |
| CANBUS-4   | 0.0                         | 0.0                         | 1.0                            |
| CANBUS-5   | 0.0                         | 0.1                         | 1.0                            |
| CANBUS-6   | 0.0                         | 0.0                         | 1.2                            |
| CANBUS-7   | 0.0                         | 0.0                         | 1.4                            |
| CANBUS-8   | 0.0                         | 0.0                         | 0.8                            |
| CANBUS-9   | 0.0                         | -0.1                        | 0.8                            |
| CANBUS-10  | 0.0                         | 0.0                         | 0.2                            |
| CANBUS-11  | 0.0                         | 0.0                         | 1.1                            |
| CANBUS-12  | 0.0                         | 0.0                         | 2.3                            |
| CANBUS-13  | 0.1                         | 0.5                         | -6.9                           |
| CANBUS-14  | 0.0                         | 0.1                         | 0.4                            |
| CANBUS-15  | 1.4                         | 6.9                         | 12.7                           |
| CANBUS-16  | 0.1                         | 0.3                         | 0.9                            |
| CANBUS-17  | 0.0                         | 0.0                         | -0.3                           |
| ECU-ACOC-1 | 1.2                         | 1.1                         | 2.5                            |
| H502-1     | 0.5                         | 0.0                         | -0.7                           |
| PBCU-FW-1  | 0.0                         | 0.0                         | 0.2                            |
| PBCU-FW-2  | 0.0                         | 0.0                         | 0.1                            |
| PBCU-FW-3  | 0.0                         | 0.0                         | 0.1                            |
| PBCU-FW-4  | 0.0                         | 0.0                         | 0.0                            |
| PBCU-FW-5  | 0.0                         | 0.0                         | 0.0                            |
| PBCU-FW-6  | 0.0                         | 0.0                         | 0.0                            |
| PBCU-FW-7  | 0.0                         | 0.0                         | 0.0                            |
| HF02       | n/a                         | n/a                         | 10.6                           |

true for cables carrying small currents; thus, the PBCU-FW-1 current is also very low, but, since it is located further away, it is less affected by modifications.

In view of these results, we conclude that not including an equipment item or system in the model could be an unwise decision, negatively affecting the assessment made of equipment in electrical contact with the equipment/system excluded.

### 3.1.2. Removal of the Inlet Particle Separator Actuator (IPSA)

The conclusions reached in the above section hold even for the removal of a small item of equipment (IPSA in Fig. 2), when its electrical connection with the cable termination under analysis is not so evident. There is no cable connecting the IPSA, but it is in contact with the OILS by means of the lower fairing, and, as observed above, the OILS, in turn, is in electrical contact with ACOC. In this case, considerable differences are also evident at CANBUS-15 and ECU-ACOC, as shown in the third column of Table 1.

Therefore, we conclude that not only must the equipment/systems in direct electrical contact with

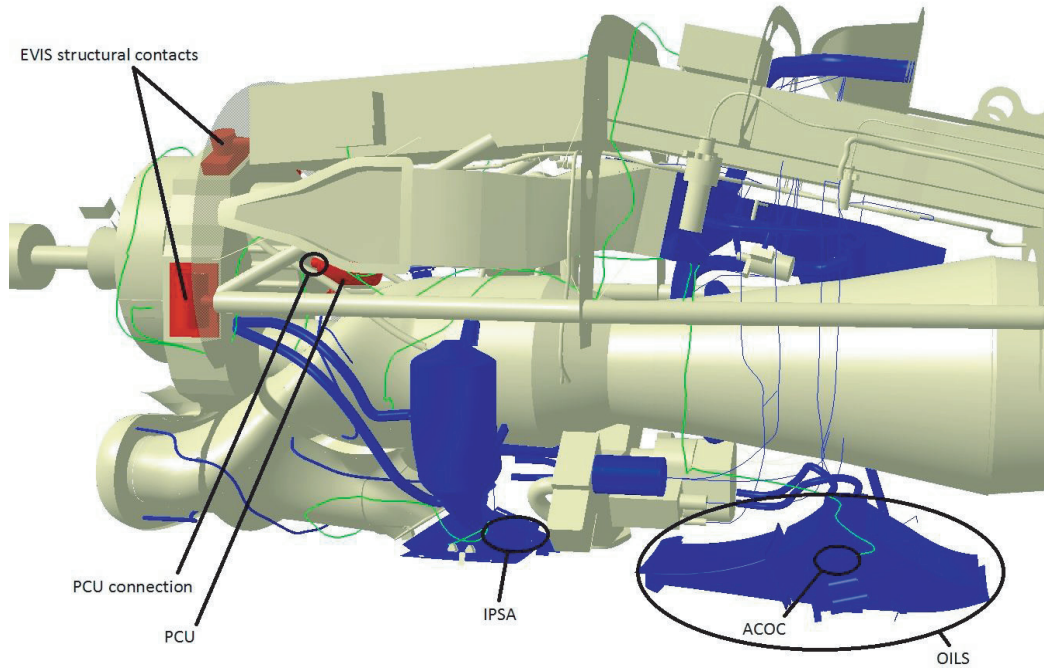


**Figure 2.** Detailed view of the EM model (some parts not shown or depicted with a degree of transparency to visualise the inner structure; systems are in dark blue and harnesses in green).

the equipment under study be included in the model, but also any equipment/system joined to it, even if this is by means of several interconnected pieces.

### 3.1.3. Removal of All Systems

In this stage of the analysis, we remove not only the OILS and IPSA but also all the systems from the model (dark blue components in Fig. 2). For the cables terminating at a system, we created a fictitious connection to minimise the degradation of the cable terminations. As expected, this modification affected more cables (see column four in Table 1), especially those with a modified connection (CANBUS-13), those that must conform to the nodal rule (CANBUS-12), and those which run close to systems bearing high currents. To justify this last assertion, we analysed the currents which run along the main systems, and added another cable to the study, HF02, which has an extension parallel to the Nacelle Bleed Air System, which bears a current flow of thousands of amperes (measured with a bulk current probe); it was observed that removing the systems severely affected this new cable.

Frequency domain analysis revealed an important change in the level of resonance at 30 MHz in the H502 cable (Fig. 3). This is not the only example as almost all cables present higher amplitudes in their initial resonances. In addition, in every cable can be seen a resonance shift towards lower frequencies (an example is shown in Fig. 4). These phenomena would modify the amplitudes and frequencies at which WF 3 should be applied during the equipment qualification tests (although the present regulation only requires qualification with a damped sinusoid of 1 and 10 MHz by default, it is recommended that the equipment should be qualified at any other frequency at which there is a known resonance) [14, 19].

In the light of these results, the model must also include any equipment/system located close to the wiring being analysed, and especially those bearing high currents.

## 3.2. Change of Electrical Contacts

The following two examples highlight the importance of correctly modelling the electrical contact between different components.

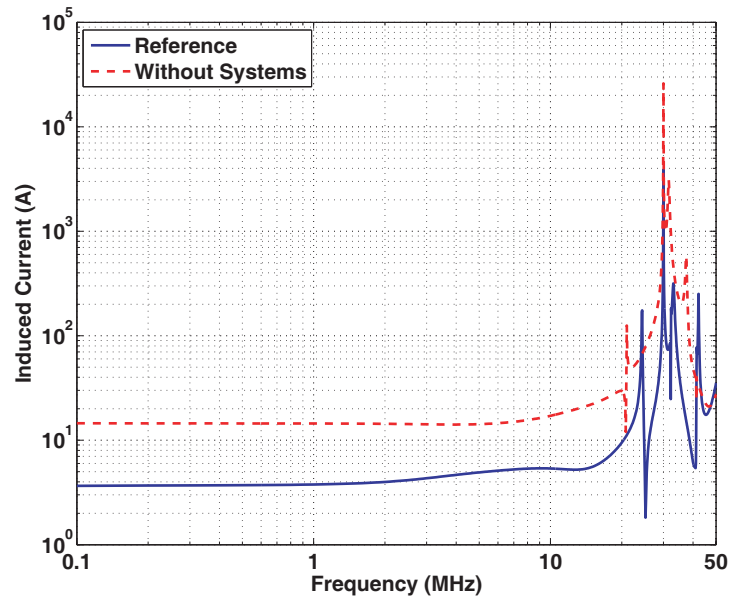


Figure 3. FFT comparison — Without systems — H502-1 harness branch.

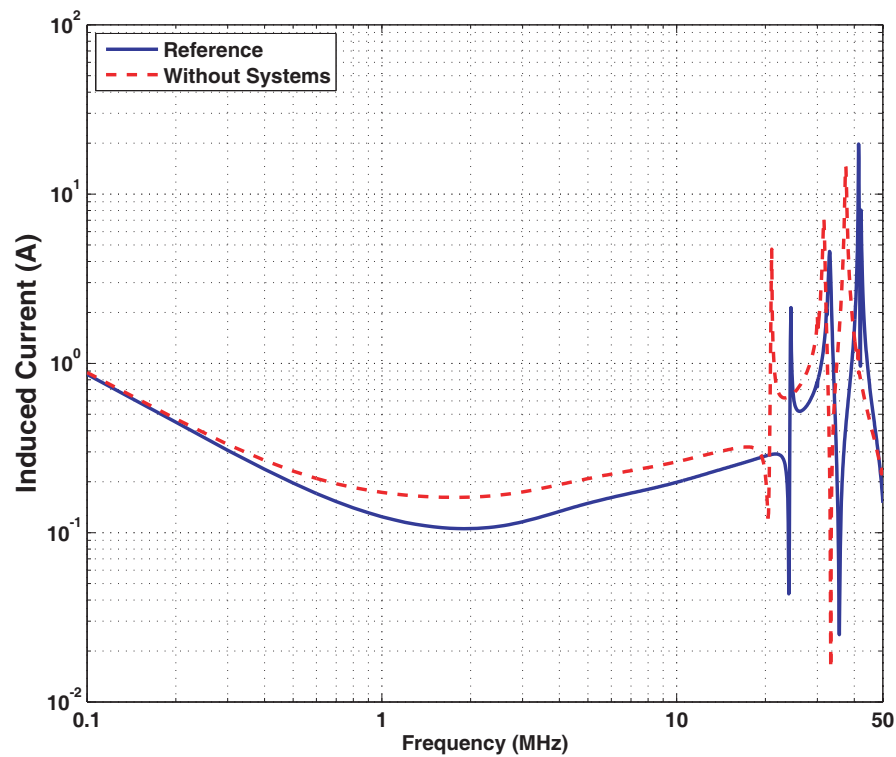


Figure 4. FFT comparison — Without systems — PBCU-FW-3 harness branch.

3.2.1. With the Electronic Vibration Isolation System (EVIS) Structural Contact

Unless we have a full mock-up including material data and comprising materials from every component, the most straightforward approach is probably to assume that two elements which are in mechanical contact are also in electrical contact. However, that is not the case when non-conductor materials are involved. Accordingly, we chose the four EVIS, which connect the engine to the mounting at the

front part of the model, but which are insulating (Fig. 2). The electrical connection is guaranteed by four bonding jumpers because the current must pass from the engine to the mounting. Nevertheless, even though there is an electrical connection, the induction diminishes if this connection is made by structural means rather than by bonding braids. As can be seen in the second column of Table 2, this is more significant for the cables that connect equipment to the engine, because of the smaller amount of current flowing through the engine. The third column in Table 2 also shows that most of the cables affected are subject to a delay in the peak time. In every cable, there is a resonance shift towards higher frequencies, as explained above, and this could lead to problems in performing the qualification with WF 3.

**Table 2.** Change of electrical contacts.

| Branch     | With EVIS Str       |                         | Without PCU Conn    |
|------------|---------------------|-------------------------|---------------------|
|            | $\Delta(\text{dB})$ | $\Delta t(\mu\text{s})$ | $\Delta(\text{dB})$ |
| CANBUS-1   | -19.6               | -0.3                    | -0.1                |
| CANBUS-2   | -19.3               | 1.3                     | 0.6                 |
| CANBUS-3   | -17.7               | 8.5                     | 1.9                 |
| CANBUS-4   | -18.8               | -0.5                    | -0.9                |
| CANBUS-5   | -18.5               | -1.4                    | -2.8                |
| CANBUS-6   | -8.1                | 0.1                     | 1.7                 |
| CANBUS-7   | -8.6                | 0.5                     | 1.7                 |
| CANBUS-8   | -6.5                | -0.7                    | 1.5                 |
| CANBUS-9   | -2.7                | 4.9                     | -5.5                |
| CANBUS-10  | -13.0               | 8.6                     | -27.9               |
| CANBUS-11  | -12.7               | 7.7                     | $-\infty$           |
| CANBUS-12  | -12.0               | 6.0                     | -22.6               |
| CANBUS-13  | -15.6               | 2.1                     | 6.6                 |
| CANBUS-14  | -13.0               | 5.1                     | -3.1                |
| CANBUS-15  | 18.2                | 14.4                    | 16.3                |
| CANBUS-16  | -15.0               | 0.9                     | -1.9                |
| CANBUS-17  | 0.0                 | 0.0                     | 0.0                 |
| ECU-ACOC-1 | -20.1               | 13.7                    | -0.5                |
| H502-1     | -2.6                | -0.4                    | 0.0                 |
| PBCU-FW-1  | 5.0                 | 17.1                    | -0.2                |
| PBCU-FW-2  | 0.5                 | -0.4                    | 0.0                 |
| PBCU-FW-3  | -0.4                | 0.3                     | 0.0                 |
| PBCU-FW-4  | 0.2                 | -0.1                    | 0.0                 |
| PBCU-FW-5  | 0.0                 | 0.1                     | 0.0                 |
| PBCU-FW-6  | 0.0                 | 0.0                     | 0.0                 |
| PBCU-FW-7  | 0.0                 | 0.0                     | 0.0                 |

There is a huge reduction in the current induced in the model with EVIS, and therefore we conclude that adding a structural contact where one does not exist, even though there is another form of electrical contact, could lead to insufficient qualification/protection, jeopardising the safety of the aircraft.

### 3.2.2. Without Propeller Control Unit (PCU) Connection

Mock-ups are usually divided into discrete zones so that it is not necessary to open up the complete model in order to see one particular item, thus reducing memory requirements. The PCU is an equipment

element which is joined to the engine by a set of cylinders (Fig. 2) represented in different zones of the mock-up. The fourth column of Table 2 shows how the currents induced would change if one of these cylinders were not included. This might happen if the zone in which it is located were not present on the screen. Not only CANBUS-11, which is the branch connected to PCU and thus in open circuit in the modified configuration, but virtually the entire harness would be affected, in order to meet the nodal rule. The error might be readily apparent if the CANBUS-11 branch is analysed; on the other hand, the PCU might be beyond of the scope of observation; nevertheless, its error would be propagated to the branches of the equipment being studied. Frequency domain results show that, even when there is no direct current flowing along CANBUS-11 (remember the  $-\infty$  obtained in the time domain), the resonance at 25 MHz strengthens (Fig. 5). In consequence, when a cable termination is disconnected, the high frequency must be considered. Simulating this equipment as being isolated would lead us to qualify the equipment with a WF 3 of high amplitude at 25 MHz, when in reality there is no reason to do so.

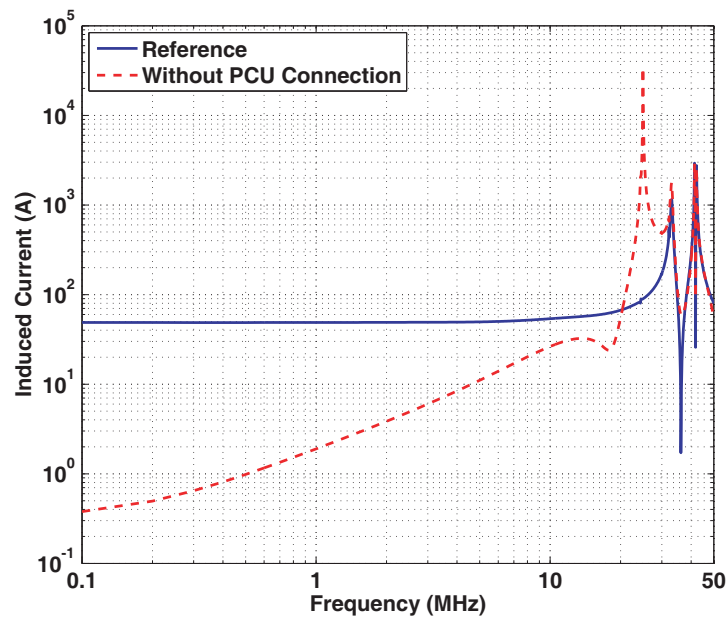


**Figure 5.** FFT comparison — Without PCU connection — CANBUS-11 harness branch.

Therefore, we conclude that the electrical contacts between the equipment and the whole model are of prime importance, so much so that if these questions were ignored, systems could be incorrectly qualified.

### 3.3. Inclusion of Non-PEC Materials

The configurations presented below were devised to enable us to analyse the consideration of materials other than perfect electric conductors (PEC).

#### 3.3.1. PEC

Most of the nacelle is made of carbon fibre, and it can be modelled using thin layer sub-cell models, as described in [34]. In the present study mean values of conductivity and thickness for the thin-layer material were assigned and no anisotropy was taken into account (conductivity of  $2.2 \cdot 10^4$  S/m and 2 mm of thickness for CFC and conductivity of  $3.3 \cdot 10^4$  S/m and 2 mm of thickness for CFC with bronze mesh). The second and third columns of Table 3 show what happens if it is modelled simply as a PEC. In general, current induction is expected to be lower, due to the better shielding effectiveness of PEC materials, which provide greater protection against lightning strikes and prevent the field leakage within

**Table 3.** Material assignation ( $\Delta$  is in db and  $\Delta t$  in  $\mu$ s).

| Branch     | PEC      |            | Lossy RefCFC |            | Lossy RefPEC |            |
|------------|----------|------------|--------------|------------|--------------|------------|
|            | $\Delta$ | $\Delta t$ | $\Delta$     | $\Delta t$ | $\Delta$     | $\Delta t$ |
| CANBUS-1   | 0.1      | 0.1        | -0.1         | -0.1       | -0.1         | 0.0        |
| CANBUS-2   | 0.0      | 0.1        | 0.0          | 0.1        | 0.0          | 0.0        |
| CANBUS-3   | -0.1     | -0.1       | 0.1          | 0.2        | 0.2          | 0.1        |
| CANBUS-4   | 0.1      | 0.2        | 0.0          | 0.1        | 0.0          | 0.2        |
| CANBUS-5   | 0.2      | 0.4        | -0.1         | 0.0        | 0.0          | 0.1        |
| CANBUS-6   | 0.0      | 0.0        | 0.0          | 0.1        | 0.0          | 0.1        |
| CANBUS-7   | 0.0      | -0.1       | 0.0          | 0.0        | 0.0          | 0.1        |
| CANBUS-8   | 0.1      | 0.3        | 0.1          | 0.1        | 0.1          | 0.1        |
| CANBUS-9   | -1.0     | -2.8       | 0.2          | 0.1        | 0.2          | 0.1        |
| CANBUS-10  | -0.3     | -0.5       | 0.0          | 0.1        | 0.1          | 0.1        |
| CANBUS-11  | -0.2     | -0.5       | 0.1          | 0.1        | 0.1          | 0.1        |
| CANBUS-12  | -0.2     | -0.4       | 0.2          | 0.0        | 0.2          | 0.0        |
| CANBUS-13  | -0.2     | -0.4       | 0.6          | 0.4        | 0.7          | 0.8        |
| CANBUS-14  | -0.2     | -0.3       | 0.3          | 0.2        | 0.3          | 0.3        |
| CANBUS-15  | 2.5      | 1.8        | 2.9          | 2.2        | 5.9          | 6.8        |
| CANBUS-16  | -0.1     | -0.1       | 0.4          | 0.3        | 0.5          | 0.5        |
| CANBUS-17  | -43.1    | -12.5      | -0.3         | 0.0        | -1.2         | -0.3       |
| ECU-ACOC-1 | 0.4      | 0.7        | -1.7         | -1.4       | -1.8         | -1.7       |
| H502-1     | -5.8     | -9.3       | 4.4          | -3.7       | 8.5          | 4.9        |
| PBCU-FW-1  | 0.0      | 1.3        | 17.1         | 13.5       | 19.6         | 11.9       |
| PBCU-FW-2  | -22.5    | -13.4      | 2.6          | -0.4       | 14.0         | 12.7       |
| PBCU-FW-3  | -28.8    | -11.4      | -5.6         | 2.6        | 26.5         | 11.6       |
| PBCU-FW-4  | -45.1    | -13.9      | 3.1          | -0.4       | 34.6         | 10.4       |
| PBCU-FW-5  | -42.3    | -12.2      | 1.2          | 0.2        | 1.9          | -2.3       |
| PBCU-FW-6  | -44.9    | -12.0      | 1.1          | 0.3        | 2.5          | -2.2       |
| PBCU-FW-7  | -40.3    | -12.4      | 1.2          | 0.2        | 1.6          | -2.3       |

the structure. On the other hand, the slight delays in the peak time that are observed in the carbon fibre nacelle, due to its electrical resistance, especially in the branches running near the fairings, that is, CANBUS-17, H502 and PBCU-FW harnesses, disappear when everything is PEC. Frequency domain results show that the induction only decreases at low frequencies, since at high frequencies the carbon fibre is close to being a PEC (Fig. 6).

### 3.3.2. Lossy Hinges

The hinges are sometimes made of fibre, in order to save weight. In this section, we study the effect of lossy hinges on protection against lightning. To do so, properties of isotropic material with a conductivity of  $10^3$  S/m were assigned to the door hinges. This modification was first carried out in the reference model, that is, with the carbon fibre nacelle. Subsequently, the same modification was performed in the completely metallic model analysed in the previous section. In both cases, lossy hinges moderately

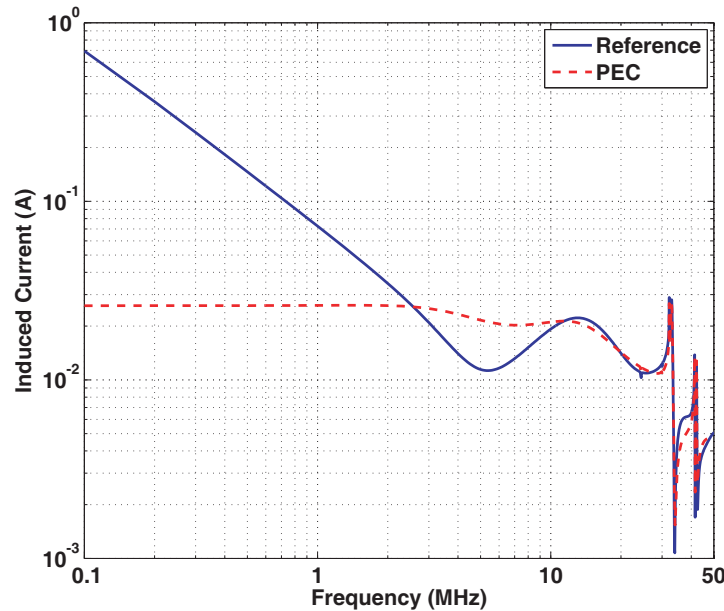


**Figure 6.** FFT comparison — PEC — CANBUS-17 harness branch.

degrade the protection provided by the fairing, mainly affecting the cables running near it, especially those with paths below carbon fibre components that are joined by hinges (see columns four to seven in Table 3). For the metallic nacelle, slight delays in the peak time were also observed. These findings suggest that simulations must be repeated when a decision regarding the material composition is to be made.

### 3.4. Cable Properties and Modifications

In this section, we examine a fourth group of modifications, to determine the influence of the cables selected for analysis, and the cable route, impedance or radius, when generating an EM model.

#### 3.4.1. Cable Addition

If another cable is added to the model, this will modify the currents induced at cables with parallel routes. Fig. 7 shows in light green a route added to the reference model, with an extension of around 0.5 m, and running parallel to the ECU-ACOC route (depicted in dark green) at a distance of 1 cm. The second column in Table 4 represents the variation in the current induced at each observable point following the introduction of this new cable which has a flow of around 3000 A. As was to be expected, only the result at the ECU-ACOC harness was affected. However, this variation means that we cannot analyse the cables as if they were isolated problems because the other cables in the model could affect the current induction. This is particularly important when there are shared routes and strong currents flowing along some cables. In this situation, a full-wave MTLN approach is used [28] to determine the currents flowing through the cable overbraids.

#### 3.4.2. Cable Displacement

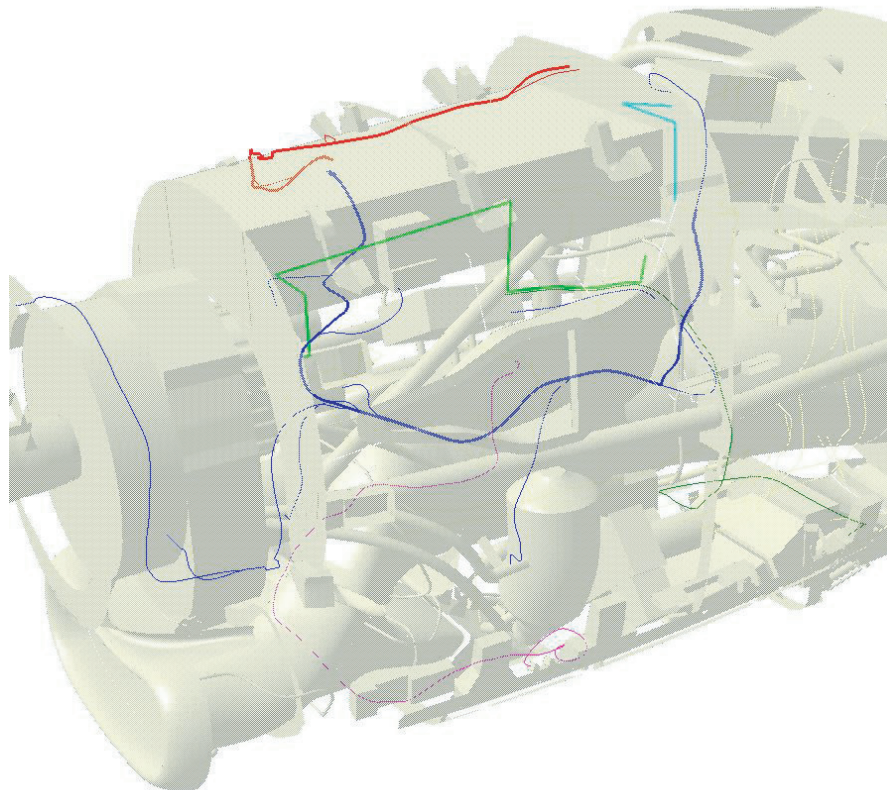
CANBUS-17 is a point to point cable which runs from the firewall to the EPMU; it is separated by the firewall from the remaining CANBUS branches. Fig. 7 shows this short cable, in cyan, displaced about 10 cm from its original route, in dark blue thin line. The third column in Table 4 shows the variation in the currents induced due to this modification. Obviously, only the CANBUS-17 harness is affected. The variation observed is significant because the loop area has been modified, meaning that the exact route of the cables must be respected in the EM model.

Table 4. Cable properties and modifications.

| Branch     | Cable modifications       |                               |                                |
|------------|---------------------------|-------------------------------|--------------------------------|
|            | Addition<br>$\Delta$ (dB) | Displacement<br>$\Delta$ (dB) | Ramifications<br>$\Delta$ (dB) |
| CANBUS-1   | -0.3                      | 0.0                           | -22.2                          |
| CANBUS-2   | -0.2                      | 0.0                           | n/a                            |
| CANBUS-3   | -0.1                      | 0.0                           | -16.8                          |
| CANBUS-4   | -0.2                      | 0.0                           | n/a                            |
| CANBUS-5   | -0.3                      | 0.1                           | -21.6                          |
| CANBUS-6   | -0.1                      | 0.0                           | n/a                            |
| CANBUS-7   | -0.1                      | 0.0                           | n/a                            |
| CANBUS-8   | -0.1                      | 0.0                           | n/a                            |
| CANBUS-9   | 0.0                       | 0.0                           | n/a                            |
| CANBUS-10  | -0.3                      | 0.0                           | -18.1                          |
| CANBUS-11  | -0.2                      | 0.0                           | n/a                            |
| CANBUS-12  | -0.1                      | 0.0                           | -14.9                          |
| CANBUS-13  | 0.4                       | 0.0                           | n/a                            |
| CANBUS-14  | 0.1                       | 0.0                           | -17.6                          |
| CANBUS-15  | 15.2                      | 0.0                           | n/a                            |
| CANBUS-16  | -0.3                      | 0.0                           | -17.7                          |
| CANBUS-17  | 0.0                       | -6.9                          | n/a                            |
| ECU-ACOC-1 | -6.3                      | 0.0                           | n/a                            |
| H502-1     | 0.0                       | 0.0                           | n/a                            |
| PBCU-FW-1  | -0.6                      | 0.0                           | 21.2                           |
| PBCU-FW-2  | 0.0                       | 0.0                           | n/a                            |
| PBCU-FW-3  | -0.1                      | 0.0                           | 3.7                            |
| PBCU-FW-4  | 0.0                       | 0.0                           | n/a                            |
| PBCU-FW-5  | 0.0                       | 0.0                           | -6.7                           |
| PBCU-FW-6  | 0.0                       | 0.0                           | n/a                            |
| PBCU-FW-7  | 0.0                       | 0.0                           | -0.6                           |

| Branch     | Connector resistances  |   |       | Pig-tails<br>$L$<br>$\Delta$ (dB) | Reduced radius       |                      |
|------------|--|---|-------|-----------------------------------|----------------------|----------------------|
|            | $R_c=10\text{ m}\Omega$<br>$R/l=10\text{ m}\Omega/\text{m}$<br>$\Delta$ (dB) | $R_c=100\text{ }\Omega$<br>$\Delta$ (dB)   $\Delta t$ ( $\mu\text{s}$ ) |       |                                   | 40%<br>$\Delta$ (dB) | 80%<br>$\Delta$ (dB) |
|            | CANBUS-1   | -0.3  | -41.2 | -5.4                              | -0.8                 | -0.8                 |
| CANBUS-2   | -0.4   | -48.2   | -5.3  | -1.1                              | -0.8                 | -2.2                 |
| CANBUS-3   | -0.5   | -42.2   | -5.3  | -1.7                              | -0.7                 | -2.1                 |
| CANBUS-4   | -0.4   | -44.1   | -5.2  | -0.9                              | -0.8                 | -2.3                 |
| CANBUS-5   | -0.3   | -37.4   | -5.2  | -0.6                              | -0.8                 | -2.4                 |
| CANBUS-6   | -0.3   | -34.0   | -5.5  | -0.4                              | -0.9                 | -2.5                 |
| CANBUS-7   | -0.3   | -37.7   | -5.6  | -0.6                              | -0.9                 | -2.5                 |
| CANBUS-8   | -0.1   | -27.6   | -5.7  | 0.3                               | -0.9                 | -2.5                 |
| CANBUS-9   | -0.4   | -44.4   | -8.2  | -0.7                              | -0.7                 | -2.1                 |
| CANBUS-10  | -0.4   | -58.4   | -5.7  | -1.0                              | -0.7                 | -2.1                 |
| CANBUS-11  | -0.3   | -42.9   | -6.0  | -0.7                              | -0.7                 | -2.1                 |
| CANBUS-12  | -0.2   | -33.9   | -6.0  | -0.4                              | -0.7                 | -1.9                 |
| CANBUS-13  | -0.3   | -42.7   | -6.0  | -0.5                              | -0.8                 | -2.3                 |
| CANBUS-14  | -0.3   | -36.4   | -5.9  | -0.4                              | -0.7                 | -2.0                 |
| CANBUS-15  | -0.6   | -15.1   | -2.6  | -7.9                              | -0.6                 | -2.1                 |
| CANBUS-16  | -0.3   | -38.9   | -5.8  | -0.5                              | -0.7                 | -2.0                 |
| CANBUS-17  | -0.9   | -64.3   | -14.4 | -1.4                              | -0.8                 | -2.2                 |
| ECU-ACOC-1 | -0.2   | -35.3   | -5.2  | -0.2                              | -0.7                 | -1.9                 |
| H502-1     | -0.5   | -39.1   | -14.8 | -0.3                              | -0.8                 | -2.4                 |
| PBCU-FW-1  | -0.2   | -37.8   | -0.4  | 1.0                               | -1.6                 | -4.9                 |
| PBCU-FW-2  | -0.4   | -55.1   | -14.8 | -0.6                              | -0.8                 | -2.4                 |
| PBCU-FW-3  | -0.2   | -50.3   | -12.8 | 0.4                               | -0.9                 | -2.5                 |
| PBCU-FW-4  | -0.9   | -63.5   | -14.5 | -1.3                              | -0.8                 | -2.4                 |
| PBCU-FW-5  | -0.6   | -54.4   | -14.2 | -0.7                              | -0.8                 | -2.4                 |
| PBCU-FW-6  | -0.7   | -56.0   | -14.1 | -0.7                              | -0.8                 | -2.4                 |
| PBCU-FW-7  | -0.6   | -55.9   | -14.3 | -0.7                              | -0.8                 | -2.4                 |



**Figure 7.** Cable modifications (added cable is in light green, displaced cable is in cyan, CANBUS without ramifications is in dark blue thick line and PBCU-FW without ramifications is in red thick line).

### 3.4.3. Suppression of Ramifications

Since aircraft wiring is very complicated, both in cable number and route complexity, it is necessary to include a minimal yet significant set of cables in the EM model for the simulation of a lightning strike against the aircraft. In general, the most severely affected types of equipment are those with cables extending over long routes, because with a short cable, no matter how much current flows along it, there is relatively little voltage drop between its terminations. However, this does not mean that we can choose the longest harness path and reject all the ramifications, because a high degree of error would be associated with this approximation if some of the neglected branches carried strong currents, for example, when passing through a more exposed zone or if they carried a large amount of direct current.

We calculated the current and voltage drop induced from the PBCU to the firewall connectors, through the CANBUS and PBCU-FW harnesses, with and without the remaining branches (Fig. 7 in dark blue and red). It can be observed that the current varies substantially (fourth column of Table 4). The voltage drop was calculated according to Ohm's law for both configurations, and in this respect, too, there is considerable variation (Table 5). In the light of these results, we conclude that ramifications must be included in the indirect effects of lightning simulations, even if they are not the immediate object of the study, especially when these ramifications carry strong currents.

### 3.4.4. Connector Resistance and Resistance Per Unit Length Influence

Typically, the first lightning simulations are performed during the design process, and, therefore, with generic values for overbraid resistances, since their real value is unknown in early stages. It makes sense, therefore, to consider whether simulations should be repeated with real overbraid resistances once they

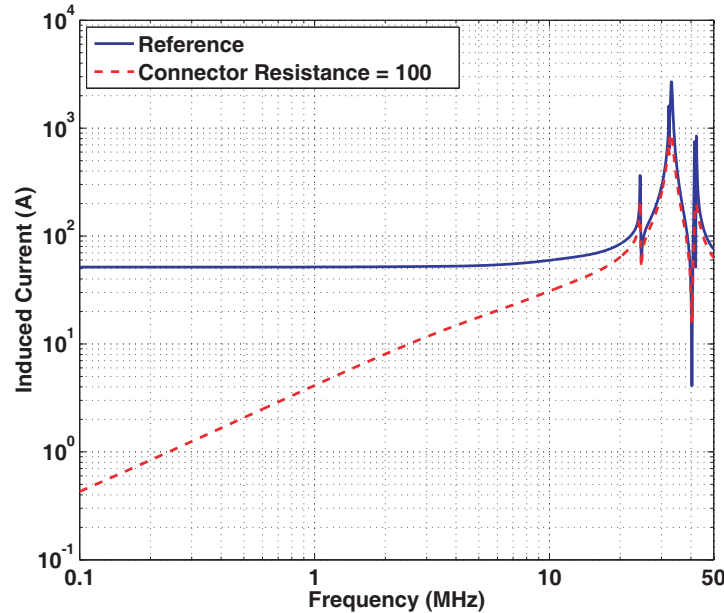
**Table 5.** Without ramifications — Voltage.

| Harness | Equipment | $\Delta_{\text{peak}}$ (dB) |
|---------|-----------|-----------------------------|
| CANBUS  | PBCU      | -5.2                        |
| PBCU-FW | PBCU      | 1.8                         |

are known. To address this question, we doubled the connector resistance (from 5 to 10 m $\Omega$ ) and the overbraid resistance per unit length (from 5 to 10 m $\Omega$ /m), which would be a reasonable variation between generic and real values. As shown in the fifth column of Table 4, the induced peak currents undergo slight variations. As expected, the most severely affected cables are CANBUS-17, because it is very short and has a connector resistance at both terminations, and the PBCU-FW harness, because its branches are very short and most of them end in a connector resistance. This study reveals that it is not necessary to repeat the simulations introducing the real resistance values provided that these are of the same order as the generic resistances used in the initial simulations.

#### 3.4.5. Equipment Isolation or High Resistance Internal Circuit

By contrast, if the items of equipment are isolated or the internal circuits at each pin have high resistances, the currents induced are completely different (see the sixth and seventh columns in Table 4 for a change from 5 m $\Omega$  to 100  $\Omega$ ). In this case, the high resistances must be considered in the simulation. Now, the peak appears more rapidly and is narrowed (that is, it presents a much lower action integral). Consequently, the DC contribution is lower but current levels are similar at higher frequencies (Fig. 8). In these circumstances, as explained above, the possible presence of strong currents at high frequencies should be taken into account in the qualification process.

**Figure 8.** FFT comparison — Connector resistance = 100  $\Omega$  — CANBUS-1 harness branch.

#### 3.4.6. Pig-Tail Termination

The connectors used for grounding the shields are usually 360-degree connector backshells, which are preferred due to their low inductance. Nevertheless, in some cases, pig-tails are used to ground the shields, and therefore we analysed the effect of those pig-tails on the currents and voltages induced. A

pig-tail inductance of 100 nH was selected, corresponding approximately to a pig-tail 10 cm long and with a diameter of 1.5 mm. Column eight in Table 4 shows the results obtained. The current variations were not so large as to modify the surrounding currents, and lower inductions were generally found. However, it is crucial to take into account the effect in the voltage induced, because the voltage drop across an inductor is proportional to the time derivative of the current, and then, this term can have a very high value.

### 3.4.7. Cable Radii

The MTLN approach of [27] is an extension of the classical Holland treatment of thin wires [18] which takes into account the coupling between parallel wires as well as that with the rest of the structure. In the Holland model, the radius of the cable impacts on the maximum time step for stability [35] and this must often be reduced in simulations in order to achieve a stable solution. In this section, we analyse the viability of this measure. To do so, we reduced the cable radius by 40% and 80% (from  $5 \cdot 10^{-4}$  m down to  $3 \cdot 10^{-4}$  m and  $1 \cdot 10^{-4}$  m, respectively). The results of these modifications are shown in Table 4, columns nine and ten. The variation in the induced current is low for the 40% reduction and substantial for 80%. However, in this latter case, the deviation was not especially alarming, in view of the dramatic reduction made in the radius. Severe reductions could be considered valid keeping a greater safety margin in the ATL. Thus, the error associated with this limitation is low and, consequently, the approximation is acceptable when the decrease is moderate, and can also be considered acceptable when larger margins are incorporated for extreme decreases in cable radius.

The results obtained can be theoretically justified taking into account the per unit length (PUL) autoinductance of a single thin wire over an indefinite ground plane in free space (Fig. 9). The distance between the wiring and the ground plane in a complex model such as a power plant is not a clean dimension, but, in this case, it takes approximately an average value of 100 times the wire radius. Making use of the equation shown in Fig. 9 for this separation value, we find that a 40% reduction in cable radius produces a current difference of  $-0.8$  dB, while an 80% reduction produces a current difference of  $-2.3$  dB, which is in agreement with the mean differences shown in columns nine and ten of Table 4.

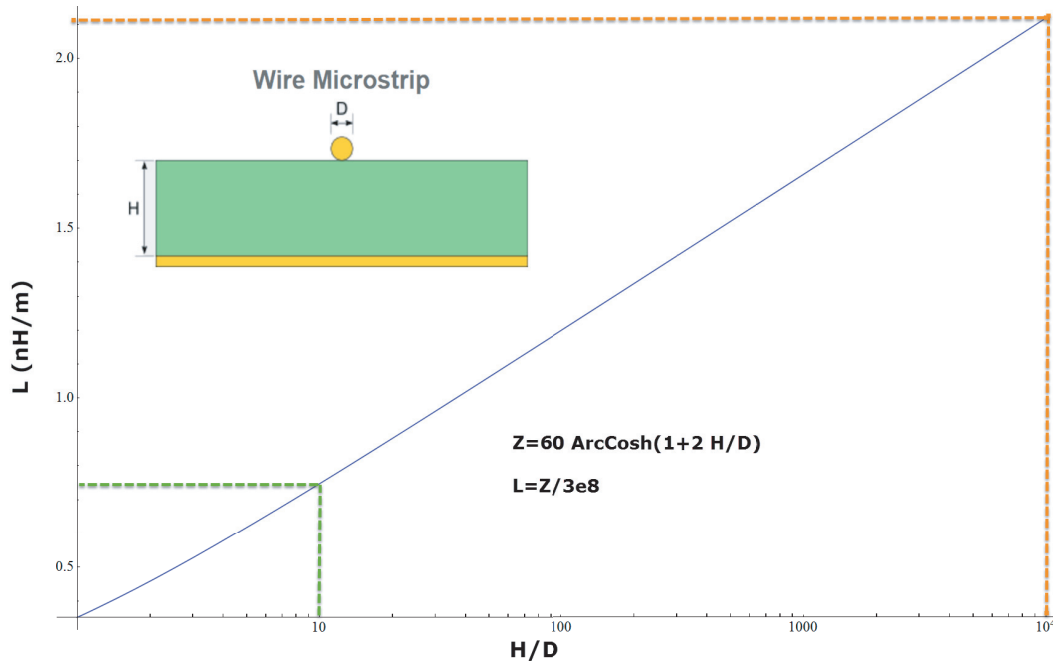


Figure 9. PUL parameters of a single thin wire over an indefinite ground plane in free space.

## 4. CONCLUSIONS

This study considers various simplifications carried out in EM modelling and quantifies their influences on the resultant ATLS. From the results obtained, we conclude that:

- It is of fundamental importance to maintain the electrical contacts in the simplified EM model in the same form as in the original.
- The model must include at least the installations/systems/equipment that are directly or indirectly connected to the wiring under analysis, and, in addition, to surrounding installations/systems/equipment when they carry strong currents.
- As the results may vary according to the materials used, different simulations must be carried out when the material composition of the structure is varied.
- Concerning the cables, there are several important considerations. First, their position must be maintained accurately. Second, surrounding cables carrying strong currents must be included, and also harness ramifications, even if they are not directly the object of the study, especially those carrying strong currents. Third, exact harness impedance values are not very important, unless they are widely different from the generic values. By contrast, the isolation of the equipment and/or connector pins must, obviously, be considered; moreover, when a cable termination is disconnected, the possible existence of strong currents at high frequencies must be taken into consideration. Finally, the use of radius values moderately lower than the real ones produces very little degradation, and can be acceptable with greater reductions if safety margins are increased.

The present paper focuses on the indirect effects detected in lightning strike simulations. The above conclusions are valid for a frequency spectrum up to around 50 MHz. Of course, a similar study could also be made for high intensity radiated fields (HIRF), i.e., those with a plane wave or antenna source covering the range from 10 kHz to 18 GHz, and the appropriate observables, in order to determine electromagnetic behaviour variations with EM model modifications with respect to this threat. For conductive effects, which are the most important ones up to 400 MHz, the cases analysed in this paper would be useful, whereas for radiated ones, the most important of which start at 100 MHz, in addition to the cases analysed in this paper. Other tests should probably be designed in order to draw the corresponding conclusions. The analysis method employed should be appropriate for this phenomenon, completely in the frequency domain and in accordance with HIRF regulation.

## ACKNOWLEDGMENT

This work has received funding from the Projects TEC2013-48414-C3-01, TEC2013-48414-C3-2-R, TEC2016-79214-C3-1-R, TEC2016-79214-C3-3-R, and TEC2015-68766-REDC (Spanish MINECO, EU FEDER), P12-TIC-1442 (J. de Andalucía, Spain), Alhambra-UGRFDTD (AIRBUS DS), and by the CSIRC alhambra.ugr.es supercomputing center.

## REFERENCES

1. Rakov, V. A. and M. A. Uman, *Lightning: Physics and Effects*, Cambridge University Press, 2003.
2. Fisher, F. A., J. A. Plumer, and R. A. Perala, *Aircraft Lightning Protection Handbook*, Federal Aviation Administration, September 1989.
3. SAE ARP 5415, rev A, February 2008 / EUROCAE ED-81 rev A1, August 1999, *User's Manual for Certification of Aircraft Electrical/Electronic Systems for the Indirect Effects of Lightning*.
4. AC 20-136B, *Protection of Aircraft Electrical/Electronic Systems against the Indirect Effects of Lightning*, September 2011.
5. Goodloe, C. C., *Lightning Protection Guidelines for Aerospace Vehicle*, NASA, May 1999.
6. Odam, G. A. M., A. W. Hanson, and R. H. Evans, *Lightning Protection Requirements for Aircraft a Proposed Specification*, Defence Research Agency, Controller HMSO London, Revised Issue 1, May 1991.

7. Uman, M. A., *The Art and Science of Lightning Protection*, Cambridge University Press, 2008.
8. Gil, E. P. and G. G. Gutierrez, "Simplification and cleaning of complex CAD models for EMC simulations," *International Symposium on Electromagnetic Compatibility EMC Europe*, York, UK, 2011.
9. Nogueira de Sao Jose, A., A. Colin, J. Fujioka Mologni, G. Maciulis Dip, U. do Carmo Resende, and S. Trindade Mordente Goncalves, "Computational savings based on three-dimensional automotive geometries' simplifications in electromagnetics simulations," *International Conference on Microwave and Optoelectronics*, Rio de Janeiro, 2013.
10. Smith, S. M. and C. Furse, "Stochastic FDTD for analysis of statistical variation in electromagnetic fields," *IEEE Transactions on Antennas and Propagation*, Vol. 60, 3343–3350, July 2012.
11. Pyrialakos, G., T. Zygiridis, N. Kantartzis, and T. Tsiboukis, "FDTD analysis of 3D lightning problems with material uncertainties on GPU architecture," *Proc. Int. Symp. Electromagnetic Compatibility*, 577–582, Sept. 2014.
12. "A400M," <http://militaryaircraft-airbusds.com/aircraft/a400m/a400mabout.aspx>.
13. "SEMBA by UGR (2013)," <http://www.sembahome.org/>.
14. EUROCAE ED-84, Septembre 1997 / SAE ARP 5412, rev A, February 2005, *Aircraft Lightning Environment and Related Test Waveforms Standard*.
15. I. Standard P1557, *Standard for Validation of Computational Electromagnetics Computer Modelling and Simulation*, Part 1, 2, 2008.
16. Duffy, A., A. Martin, A. Orlandi, G. Antonini, T. Benson, and M. Woolfson, "Feature Selective Validation (FSV) for validation of Computational Electromagnetics (CEM). Part I — The FSV method," *IEEE Transactions on Electromagnetics Compatibility*, Vol. 48, No. 3, 449–459, August 2006.
17. Orlandi, A., A. Duffy, B. Archambeault, G. Antonini, D. Coleby, and S. Connor, "Feature Selective Validation (FSV) for validation of Computational Electromagnetics (CEM). Part II — Assessment of FSV performance," *IEEE Transactions on Electromagnetics Compatibility*, Vol. 48, No. 3, 460–467, August 2006.
18. Holland, R. and L. Simpson, "Finite-difference analysis of EMP coupling to thin struts and wires," *IEEE Transactions on Electromagnetic Compatibility*, No. 2, 88–97, 1981.
19. RTCA/DO-160, issue G, December 2010 / EUROCAE ED-14, issue G, May 2011, *Environmental Conditions and Test Procedures for Airborne Equipment*.
20. Serway, R. A. and J. W. Jewett, Jr., *Principles of Physics*, Brooks/Cole, 2013.
21. Mur, G., "Absorbing boundary conditions for the finite-difference approximation of the time-domain electromagnetic-field equations," *IEEE Transactions on Electromagnetic Compatibility*, Vol. 23, 377–382, November 1981.
22. Taflove, A. and S. Hagness, *Computational Electrodynamics: The Finite-Difference Time-Domain Method*, Artech House, Norwood, MA, 2005.
23. "CATIA by Dassault Systemes," <http://www.3ds.com>.
24. "CADfix," <http://www.transcendata.com/products/cadfix/>.
25. Garcia, S. G., J. Alvarez, L. D. Angulo, and M. R. Cabello, "UGRFDTD EM solver," <http://www.sembahome.org/>.
26. Yee, K. S., "Numerical solution of initial boundary value problems involving Maxwell's equations in isotropic media," *IEEE Transactions on Antennas and Propagation*, Vol. 14, No. 3, 302–307, 1966.
27. Berenger, J.-P., "A multiwire formalism for the fdtd method," *IEEE Transactions on Electromagnetic Compatibility*, Vol. 42, No. 3, 257–264, 2000.
28. "HIRF-SE project (2008)," <http://hirfse.axessim.eu/>.
29. "Alhambra-UGRFDTD by CSIRC (2013)," <https://alhambra.ugr.es/>.
30. Romero, S. F., G. G. Gutierrez, A. L. Morales, and M. A. Cancela, "Validation procedure of low level coupling tests on real aircraft structure," *International Symposium on Electromagnetic Compatibility EMC Europe*, 2012.

31. Gutierrez, G. G., J. Alvarez, E. Pascual-Gil, M. Bandinelli, R. Guidi, V. Martorelli, M. F. Pantoja, M. R. Cabello, and S. G. Garcia, "HIRF virtual testing on the C-295 aircraft: On the application of a pass/fail criterion and the FSV method," *IEEE Transactions on Electromagnetic Compatibility*, Vol. 56, No. 4, 854–863, 2014.
32. Gutierrez, G. G., D. M. Romero, M. R. Cabello, E. Pascual-Gil, L. D. Angulo, and S. G. Garcia, "On the design of aircraft electrical structure networks," *IEEE Transactions on Electromagnetic Compatibility*, Vol. 2, No. 58, 401–408, 2016.
33. Gutierrez, G. G., S. F. Romero, J. Alvarez, S. G. Garcia, and E. P. Gil, "On the use of FDTD for HIRF validation and certification," *Progress In Electromagnetics Research Letters*, Vol. 32, 145–156, 2012.
34. Cabello, M. R., L. D. Angulo, J. Alvarez, I. Flintoft, S. Bourke, J. Dawson, R. G. Martin, and S. G. Garcia, "A hybrid crank-nicolson fdtd subgridding boundary condition for lossy thin-layer modeling," *IEEE Transactions on Microwave Theory and Techniques*, Vol. 65, 1397–1406, 2017.
35. Schmidt, S. and G. Lazzi, "Use of the FDTD thin-strut formalism for biomedical telemetry coil designs," *IEEE Transactions on Microwave Theory and Techniques*, Vol. 52, No. 8, 1952–1956, 2004.